

DOI: 10.1002/ange.200600356

Bioconjugated Ag Nanoparticles and CdTe Nanowires: Metamaterials with Field-Enhanced Light Absorption***Jaebeom Lee, Tanveer Javed, Timur Skeini, Alexander O. Govorov, Garnett W. Bryant, and Nicholas A. Kotov**

The hybrid assembly of inorganic and metallic nanomaterials by means of chemical and biological bonding to yield manifold optical and electromagnetic properties has received widespread attention.^[2-11] Currently available highly monodispersed nanomaterials such as semiconductors and noble metals that can be conjugated by ligand-receptor, antigen-antibody reactions, polymer tethering, and DNA hybridization are used as building blocks for 2D or 3D superstructures in which new collective properties of these artificial assemblies have been obtained.^[12-15] They represent a large class of new materials (i.e., metamaterials) in which the properties are determined not only by classical atomic composition, but also by nanoscale organization of structural components. Recently, metamaterials based on metallic composites have received special attention as these are expected to display negative values for permittivity and refractive index. This property should lead to a multitude of unique optical effects.^[11,16,17] Many of these effects are related to surface plasmons on Au or Ag nanoparticles (NPs), which generate exceptionally high localized electromagnetic fields, and have been exploited in surface-enhanced Raman spectroscopy^[18-21] and some optoelectronic devices.^[12,22] Metamaterials from semiconductors and their combinations with metals can also produce optical effects that are useful for development of advanced sensing and imaging technologies.^[23,24] Recently, we

[*] Dr. J. Lee, Prof. Dr. N. A. Kotov
Department of Chemical Engineering
Department of Materials Science and Engineering and
Department of Biomedical Engineering
University of Michigan
Ann Arbor, MI 48109 (USA)
Fax: (+1) 734-764-7454
E-mail: kotov@umich.edu
T. Javed, T. Skeini, Prof. Dr. A. O. Govorov
Department of Physics and Astronomy
Ohio University
Athens, OH 45701 (USA)
Dr. G. W. Bryant
Quantum Processes and Metrology Group
National Institute of Standards and Technology
Atomic Physics Division
100 Bureau Drive, Stop 8423
Gaithersburg, MD 20899-8423 (USA)

[**] This work was supported in part by NSF Biophotonics and NSF CAREER at UM, and NIST and BNNT initiative at OU.



Supporting information for this article is available on the WWW under <http://www.angewandte.org> or from the author.

observed that the collective plasmon resonance in a specially designed assembly of Au NPs can stimulate radiative recombination of excitons in CdTe NPs and nanowires (NWs). For example, the bioconjugates of Au NPs and CdTe NWs assembled with streptavidin (SA) and D-biotin (B) exhibited fivefold enhancement of luminescence and blue shifts of emission bands. Modeling studies showed that the luminescence enhancement originates from amplification of electromagnetic fields induced by Au NPs in the vicinity of CdTe NWs.^[1,25] Other experiments with Au and CdTe NPs in which polymer linkers were used to produce a dynamically conjugated system proved that the interaction between surface plasmons and excitons is a substantial factor in the different ratios of luminescence enhancements obtained. This interaction was dynamically modified by the reversible swelling and deswelling of the polymeric spacers inside the assembled nanoscale superstructures.^[26]

Herein, we report new superstructures based on Ag NPs. Although collective interactions between NPs and NWs in the superstructures are also important for Au NPs, the mechanism for the enhancement of the emission of the Ag-NP conjugates is qualitatively different from that of Au-based NW-NP metamaterials.^[1,25,26] In the latter, the emission enhancement comes mostly from the increase of the photon emission that is stimulated by resonance with plasmon oscillations in the NP. However, when Au is replaced with Ag, the emission enhancement comes from the increase in absorption.

A theoretical model for the experiments describes collective plasmon excitations in the Ag-NP shell and provides an accurate explanation of the optical properties of Ag-based NP-NW superstructures. This paper investigates the mechanisms of interactions between NPs and develops the understanding of such hybrid materials, which could be used for a novel class of sensors and actuators with enhanced optical and thermal properties.^[1,25]

Morphological characterization of each component of the superstructure was carried out by high-resolution transmission electron microscopy (HRTEM) and atomic force microscopy (AFM). From AFM images, the average diameters of Ag NPs and CdTe NWs were measured to be 3.11 ± 1.2 nm and 8.09 ± 2.3 nm, respectively (see the Supporting Informa-

tion). The NWs were assembled from 3.7-nm CdTe NPs according to a procedure described elsewhere (>98% yield).^[27] The NWs had an average length of 1400 ± 128 nm (with an aspect ratio of 173) and luminesced at 658 ± 2 nm. It is known that bulk Ag film has a (111) lattice spacing of 0.2359 nm. The Ag NPs have a lattice spacing of 0.235 ± 0.003 nm, which corresponds to the spacing between (111) planes of Ag crystals.^[28] The TEM image showed the Ag NPs attached to the surface or in the vicinity of a CdTe NW to form a fuzzy shell (Figure 1a). There was a noticeable red shift in UV/Vis absorption peak after attachment of proteins to the Ag NPs (Figure 1b, i→ii); this shift correlates very well with the change of dielectric constant.^[29,30]

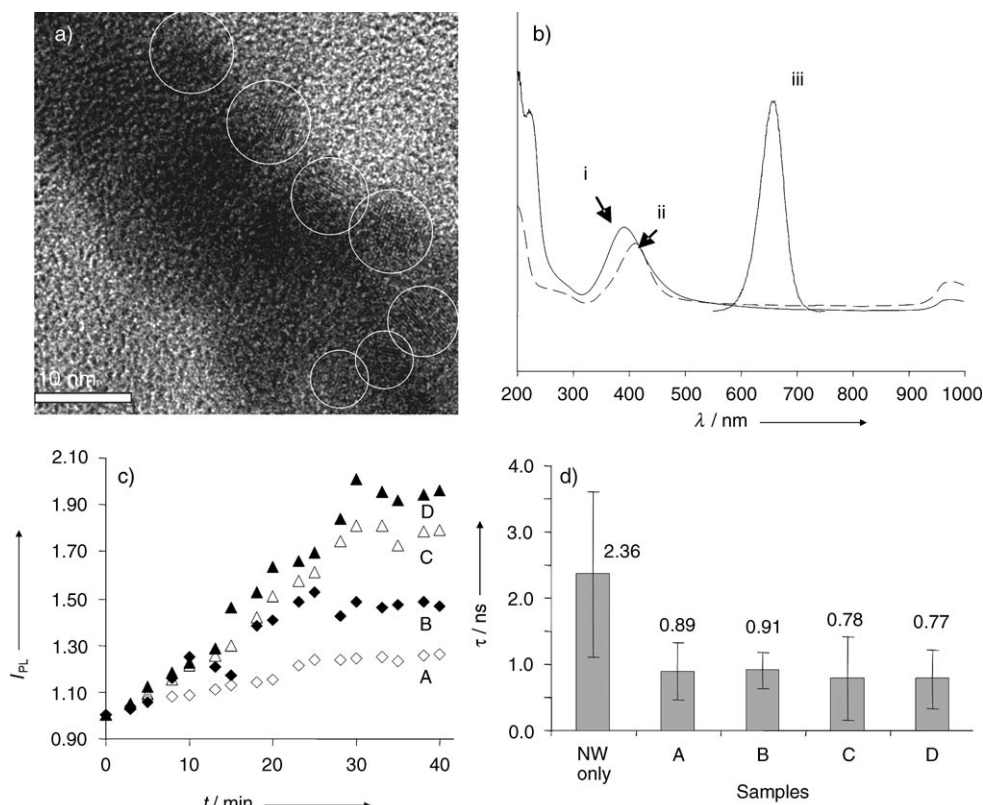


Figure 1. a) TEM image of bioconjugates of NPs and NWs, 300000 \times , b) UV/Vis and luminescence spectra of Ag NPs and CdTe NWs; i: Ag NPs, ii: Ag NPs with SA, iii: PL of NWs; c) Time courses of the luminescence peak intensities for solutions A to D. d) PL lifetimes of the respective samples.

The superstructures of Ag NPs and CdTe NWs were obtained by combining appropriate volumes of two stock solutions (NP-SA and NW-B; SA: streptavidin, B: D-biotin). The approximate molarities of the Ag NP and CdTe NW stock solutions were 2.7×10^{-6} and 2.95×10^{-9} M, respectively. The formation reaction of the NP-NW assemblies took place in 3 mL of water at pH 9 (pH adjusted with 0.1 M NaOH) in a quartz optical cuvette. Solutions were prepared with different aliquots of Ag NP dispersion (20–100 μ L) and a constant volume of the CdTe NW dispersion (20 μ L). The NP/NW ratios for the different superstructures are given in Table 1.^[1]

The intensity of the NW emission steadily increased up to twofold and the peak wavelengths were blue-shifted by up to

Table 1: Composition of different NW–NP assemblies prepared from different volume ratios of the stock NW-B and NP-SA dispersions. An averaged NW length of 1400 nm was used for calculation.

	Solution A	Solution B	Solution C	Solution D
volume ratio (CdTe NW/Au NP)	20:20	20:40	20:80	20:100
NP/NW ratio	4468	8936	17872	22340

10 nm during the bioconjugation process; these changes are smaller than those for the analogous reaction with Au NPs (see the Supporting Information).^[1] The bioconjugation of ligand receptors with attached nanocolloids was completed in approximately 30 minutes for different molar ratios of CdTe NWs and Ag NPs (Figure 1c). The photoluminescence (PL) lifetime was about 2.36 ns for the NWs alone, but decreased to around 0.84 ns for the Ag-conjugated NWs (Figure 1d). The PL intensity after that period was considered the ultimate fluorescence intensity and the assembly process was considered to reach saturation. The kinetics of the luminescence intensity is well-correlated with the conjugation of SA and B involving nanocolloids.^[1,31,32] Higher PL intensities at saturation were observed for higher NP/NW ratios (Figure 1c). The spectra of the Ag NP–NW superstructures appear similar to those of Au NP–NW superstructures, and this was initially explained on the basis of exciton–plasmon interactions.^[1] However, the underlying mechanism is essentially different. A strong indication of this is that the plasmon-resonance peak of the Ag particles does not overlap in any way with the emission peak of the NWs (Figure 1b), which is required for resonance.

The answer to this apparent discrepancy between the expected mechanism and the experimental results was found in the excitation spectra (Figure 2). As the superstructure

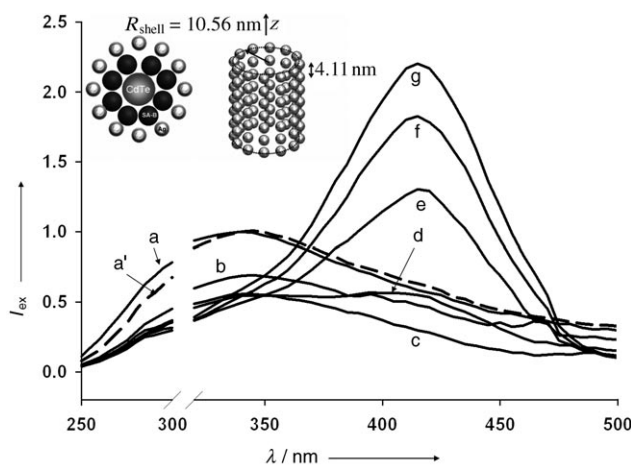


Figure 2. Photoluminescence excitation spectra of conjugated superstructures: spectra of Ag-conjugated NWs recorded every 10 minutes (a–g) for an emission wavelength of 660 nm (solution D); Au-conjugated NWs after 60 minutes (a', dashed line). The gap at 300 nm corresponds to the strong $\lambda/2$ peak of the excitation light, removed from the spectra for clarity. Inset: Cross section of the superstructure of Ag NPs, SA–B linkers, and an NW (left). Theoretical model (right) of an Ag shell with periodicity along the cylinder axis. The electromagnetic field is calculated at the center of the Ag-NP shell.

forms over a period of 20–30 min, a new feature develops in the vicinity of 420 nm. Importantly, no change is observed at this same wavelength over a period of 60 min in an experiment with the Au-conjugated NW superstructures under the same conditions (spectrum a'). Firstly, this correlates very well with the plasmon–exciton resonance mechanism suggested previously for Au NP–NW superstructures.^[32] Secondly, the excitation peak that develops at 420 nm for Ag NP–NW superstructures indicates that absorption increases drastically at this wavelength, with the energy eventually channeled into the emission of the NW at 600 nm. Thus, the reason for increase in luminescence of the Ag NP–NW superstructures is stimulated light absorption rather than light emission. The absorption of the CdTe NWs is enhanced at the exciton wavelength as a result of the proximity of the Ag NPs, which have a plasmon band that can oscillate in resonance with the exciton in the semiconductor.

To confirm this hypothesis, we calculated the electric fields inside a superstructure. The theoretical model incorporates an NW, an Ag-NP shell, and SA–B biolinkers (Figure 2, left inset). The radii of the components are taken as follows: $R_{\text{NW}} = 4$ nm, $R_{\text{SA-B}} = 2.5$ nm, and $R_{\text{AgNP}} = 1.56$ nm. The corresponding radius of the Ag-NP shell R_{shell} is 10.56 nm. The emission intensity of the superstructure is proportional to the factor $P_{\text{emiss}}(\lambda_{\text{excitation}}, \lambda_{\text{emiss}})$ [Eq. (1)], whereby $\lambda_{\text{excitation}}$ and λ_{emiss} are the excitation and exciton peak wavelengths and $P_{\text{field}}(\lambda)$ is the electric-field enhancement factor at a particular wavelength [Eq. (2)]. In Equation (2), E_0 is the amplitude of the external electric field, and E_{tot} is the resultant field in the center of the Ag-NP shell. The squared resultant electric field is averaged over all solid angles. Although the position of NPs with respect to the NW are assumed to be constant and unaffected by tumbling in solution, this assumption is necessary to account for the fact that the NWs in a solution may have variable orientation with respect to the electric field of incident light.

$$P_{\text{emiss}}(\lambda_{\text{excitation}}, \lambda_{\text{emiss}}) = P_{\text{field}}(\lambda_{\text{excitation}}) P_{\text{field}}(\lambda_{\text{emiss}}) \quad (1)$$

$$P_{\text{field}}(\lambda) = \frac{\langle E_{\text{tot}}^2 \rangle_{\Omega}}{E_0^2} \quad (2)$$

Figure 3 shows numerical simulations of the factors $P_{\text{emiss}}(\lambda_{\text{excitation}}, \lambda)$ and $P_{\text{field}}(\lambda)$ at the center of the Ag-NP superstructure (Figure 2, right inset) with Maxwell equations (see the Supporting Information). For the curves in Figure 3b, we fixed the excitation wavelength ($\lambda_{\text{excitation}} = 420$ nm) and varied the emission wavelength (λ). The data were obtained for three superstructures with total numbers of NPs $N_{\text{tot}} = 56$, 84, and 112. Each superstructure has seven rings, and the inter-ring spacing was taken as 4.11 nm. The corresponding numbers of NPs per ring (N_{ring}) were 8, 12, and 16. Note that the above numbers are less than the maximum possible number of Ag NPs per ring (i.e., 21). The corresponding linear densities of NPs were then calculated as $N_{\text{ring}}/4.11$ nm ≈ 1.95 , 2.92, and 3.89 nm⁻¹. If we now assume that total length of the NW is 1400 nm and calculate the total numbers of attached NPs using the above linear densities, we obtain 3610,

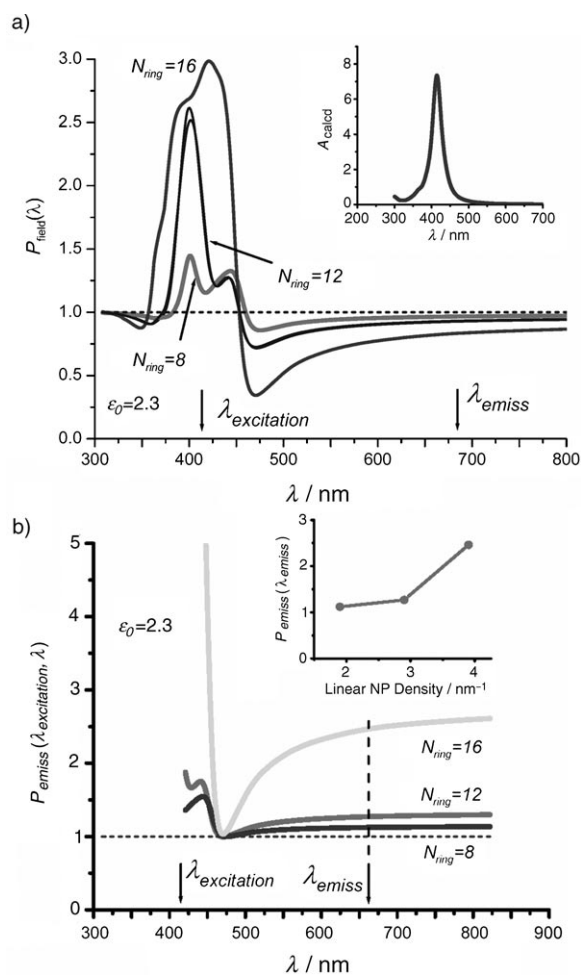


Figure 3. a) Field-enhancement factor for three superstructures with linear NP densities of 1.95, 2.92, and 3.89 nm⁻¹. Inset: Calculated absorption by a single Ag NP. The position of the plasmon resonance corresponds well with the experimental data (Figure 1b). The two curves for the 12-NP rings correspond to $l_{\max} = 1$ and 2 (l is the spherical harmonic index); the differences are minimal. b) Emission-enhancement factor as a function of the emission wavelength for three superstructures with linear NP densities of 1.95, 2.92, and 3.89 nm⁻¹; the excitation wavelength is taken as 420 nm. Inset: Calculated emission-enhancement factor at an emission wavelength of 660 nm.

5510, and 7391. These numbers are comparable to the NP/NW ratios for solutions A and B (Table 1).

The calculations demonstrate (Figure 3a) that the strength of the collective plasmon field increases gradually with increasing density of metal NPs in the shell. The spectral characteristic (energy) of the collective plasmons resonating between many Ag particles in the NP shell of the superstructure becomes wider. The factor $P_{\text{field}}(\lambda)$ is strongly enhanced for $\lambda_{\text{excitation}}$ between 400 and 450 nm and slightly reduced for λ_{emiss} at around 660 nm; thus the probability of photon emission at 660 nm in Ag-based structures is not increased but rather is even reduced slightly as a result of dynamic screening inside the shell (Figure 2, inset a). For higher density of NPs, the plasmon peak is located around 425 nm, which is red-shifted relative to the spectrum of

individual particles. This shift is illustrated by a comparison of the plasmon resonance in the Ag-NP shell (Figure 3a) with the plasmon peak of a single Ag NP (Figure 3a, inset). Again, this change results from the formation of collective plasmon resonance in the Ag-NP shell. This change is in exactly the same spectral region in which the new peak develops in the excitation spectrum (Figure 2). The nice match of the experimental results and calculations demonstrates the validity of the hypothesis of the enhanced absorption.

Some shortening of exciton lifetime of the Ag-based superstructures is observed, as was the case for Au-based superstructures (Figure 1d), although the difference is far less drastic. This effect is attributed mostly to exciton-energy dissipation in the metal. This difference between Au- and Ag-based structures is the position of the plasmon resonance with respect to the exciton energy in the CdTe NWs. In the Au-CdTe complex, the exciton energy is close to the Au plasmon peak. In the Ag-based system, the plasmon resonance is relatively far from the exciton peak. Moreover, the electric field from Ag NPs might activate some other decay mechanisms, such as nonradiative recombination pathways, which are likely to contribute to the reduced lifetime as well.

To evaluate the emission-enhancement effect qualitatively, we calculated the emission-enhancement factor $P_{\text{emiss}}(\lambda_{\text{excitation}}, \lambda)$ for the emission wavelengths $\lambda > \lambda_{\text{excitation}}$ (Figure 3b). In the experimentally important region around $\lambda_{\text{emiss}} = 660$ nm, the factor $P_{\text{emiss}}(\lambda_{\text{excitation}}, \lambda)$ increases rapidly with the number of attached NPs (Figure 3b, inset). The theoretical factor $P_{\text{emiss}}(\lambda_{\text{excitation}}, \lambda)$ for a linear NP density of 2.9 nm⁻¹ is more than 2, which is very similar to actual fluorescence enhancement in Figure 1c. The theoretical estimate from Figure 3b (2.5) also compares well with the experimental value of $P_{\text{emiss}}(\lambda_{\text{excitation}}, \lambda) \approx 3.4$ (derived in the Supporting Information). Thus, the idealized model presented herein gives a very good description of the processes in NP-NW superstructures and metal-semiconductor metamaterials.

In conclusion, we observed a twofold enhancement of luminescence intensity in the nanoscale bioconjugated superstructures made from CdTe NWs and Ag NPs. Theoretical calculations of the electric field in the cylindrically organized NPs and experimental data suggest that the enhancement in emission originates from the increase in absorption of the Ag-NP shells in the regime of the collective plasmon resonance. This situation is qualitatively different from the PL enhancement in the Au-NP/NW system studied previously. The fundamental importance of these findings is twofold: 1) The results demonstrate metamaterials for which the spatial organization of metal particles has direct consequences on the optical properties as a result of the collective nature of interactions. 2) The described calculation method can be used to predict properties of nanoscale superstructures. From a practical point of view, the combination of Au and Ag NPs may lead to the enhancement of both absorption and emission in semiconductor nanostructures, which could be utilized in a variety of optoelectronic or energy-conversion devices, for example, in solar-energy devices.

Experimental Section

CdTe NPs and NWs were prepared as described in detail elsewhere.^[27,34] Ag NPs were synthesized in solution from AgNO₃ (Aldrich^[35]), soluble starch (Aldrich^[35]), and D-glucose (Aldrich^[35]).^[36] Ethylene dichloride (EDC) and sulfo-*N*-hydroxysuccinimide (NHS) were used as zero-length cross-links to bind the inorganic and biological materials covalently (Ag NPs with streptavidin (SA), CdTe NWs with D-biotin).^[1,37] Ag NPs were bioconjugated with SA as follows: unbound starches in the Ag-NP solution were removed by repeated centrifugation and redispersion until a clear and transparent Ag-NP solution was obtained. An Ag-NP dispersion (1 mL) was mixed with thioglycolic acid (8.7 μM) for 24 h. The EDC and NHS procedures were followed to activate the carboxylic acid groups. Spectra of the bioconjugates were measured with a UV/Vis spectrophotometer (Agilent, Model-8453^[35]). The luminescence and excitation spectra of the NP–NW dispersions were measured on a Fluoromax-3 spectrofluorometer (Jobin Yvon/SPEX Horiba^[35]) every 1–2 minutes for up to 40 minutes. Atomic force microscopy (AFM)^[35] and JEOL 2010F TEM^[35] (with an accelerator voltage of 200 kV) were used to observe the morphology of the bioconjugates of Ag NPs and CdTe NWs. The lifetimes of the respective nanomaterials were measured with a Fluorolog Tau-3 (Jobin Yvon/SPEX Horiba^[35]).

Received: January 26, 2006

Published online: June 27, 2006

Keywords: bioconjugation · luminescence · metamaterials · nanotechnology · silver

- [1] J. Lee, A. O. Govorov, J. Dulka, N. A. Kotov, *Nano Lett.* **2004**, *4*, 2323–2330.
- [2] E. Prodan, C. Radloff, N. J. Halas, P. Nordlander, *Science* **2003**, *302*, 419–422.
- [3] X. Michalet, F. Pinaud, T. D. Lacoste, M. Dahan, M. P. Bruchez, A. P. Alivisatos, S. Weiss, *Single Mol.* **2001**, *2*, 261–276.
- [4] J. Zhang, N. Coombs, E. Kumacheva, Y. Lin, E. H. Sargent, *Adv. Mater.* **2002**, *14*, 1756–1759.
- [5] Z. Li, R. Jin, C. A. Mirkin, R. L. Letsinger, *Nucleic Acids Res.* **2002**, *30*, 1558–1562.
- [6] S. Westenhoff, N. A. Kotov, *J. Am. Chem. Soc.* **2002**, *124*, 2448–2449.
- [7] G. P. Goodrich, M. R. Helfrich, J. J. Overberg, C. D. Keating, *Langmuir* **2004**, *20*, 10246–10251.
- [8] J. Jiang, K. Bosnick, M. Maillard, L. Brus, *J. Phys. Chem. B* **2003**, *107*, 9964–9972.
- [9] K. Kneipp, Y. Wang, H. Kneipp, L. T. Perelman, I. Itzkan, R. R. Dasari, M. S. Feld, *Phys. Rev. Lett.* **1997**, *78*, 67–1670.
- [10] M. Maillard, P. Huang, L. Brus, *Nano Lett.* **2003**, *3*, 11–1615.
- [11] S. Riikonen, I. Romero, F. J. Garcia de Abajo, *Phys. Rev. B* **2005**, *71*, 5104.
- [12] I. Willner, B. Willner, *Pure Appl. Chem.* **2002**, *74*, 73–1783.
- [13] A. L. Rogach, *Angew. Chem.* **2003**, *115*, 150–151; *Angew. Chem. Int. Ed.* **2003**, *42*, 148–149.
- [14] Y. Lin, H. Skaff, T. Emrick, A. D. Dinsmore, T. P. Russell, *Science* **2003**, *299*, 226–229.
- [15] S. Chen, K. Kimura, *Chem. Lett.* **1999**, 233–234.
- [16] E. V. Shevchenko, D. V. Talapin, S. O'Brien, C. B. Murray, *J. Am. Chem. Soc.* **2005**, *127*, 8741–8747.
- [17] S. Zhang, W. Fan, N. C. Panou, K. J. Malloy, R. M. Osgood, S. R. J. Brueck, *Phys. Rev. Lett.* **2005**, *95*, 137404.
- [18] T. Vo-Dinh, *Trends Anal. Chem.* **1998**, *17*, 557–582.
- [19] K. G. Thomas, P. V. Kamat, *Acc. Chem. Res.* **2003**, *36*, 888–898.
- [20] Y. C. Cao, R. Jin, C. A. Mirkin, *Science* **2002**, *297*, 1536–1540.
- [21] S. Link, M. A. El Sayed, *Annu. Rev. Phys. Chem.* **2003**, *54*, 331–366.
- [22] A. N. Shipway, E. Katz, I. Willner, *ChemPhysChem* **2000**, *1*, 18–52.
- [23] J. D. Baena, R. Marques, F. Medina, J. Martel, *Phys. Rev. B* **2004**, *69*, 014402.
- [24] R. Marques, F. Medina, R. Rafii-El-Idrissi, *Phys. Rev. B* **2002**, *65*, 144440.
- [25] A. O. Govorov, W. Zhang, T. Skeini, H. Richardson, J. Lee, N. A. Kotov, *Nanoscale Res. Lett.* **2005**, *1*, 100101.
- [26] J. Lee, A. O. Govorov, N. A. Kotov, *Angew. Chem.* **2005**, *117*, 7605–7608; *Angew. Chem. Int. Ed.* **2005**, *44*, 7439–7442.
- [27] Z. Tang, N. A. Kotov, M. Giersig, *Science* **2002**, *297*, 237–240.
- [28] Z. Liu, H. Li, H. Wang, D. Shen, X. Wang, P. F. A. Alkemade, *J. Mater. Res.* **2000**, *15*, 1245–1247.
- [29] L. M. Liz-Marzan, P. Mulvaney, *J. Phys. Chem. B* **2003**, *107*, 7312–7326.
- [30] H. C. van de Hulst, *Light Scattering by Small Particles*, John Wiley & Sons, New York, **1957**, p. 470.
- [31] R. M. Penner, *J. Phys. Chem. B* **2002**, *106*, 3339–3353.
- [32] J. Lee, A. O. Govorov, N. A. Kotov, *Nano Lett.* **2005**, *5*, 2063–2069.
- [33] E. D. Palik, *Handbook of Optical Constants of Solids*, Academic Press, Orlando, **1985**, p. 804.
- [34] N. Gaponik, D. V. Talapin, A. L. Rogach, K. Hoppe, E. V. Shevchenko, A. Kornowski, A. Eychmueller, H. Weller, *J. Phys. Chem. B* **2002**, *106*, 7177–7185.
- [35] Certain commercial equipment, instruments, or materials are identified in this paper to specify the experimental procedure adequately. Such identification is not intended to imply recommendation or endorsement by the National Institute of Standards and Technology, nor is it intended to imply that the materials or equipment identified are necessarily the best available for the purpose.
- [36] P. Raveendran, J. Fu, S. L. Wallen, *J. Am. Chem. Soc.* **2003**, *125*, 13940–13941.
- [37] N. N. Mamedova, N. A. Kotov, A. L. Rogach, J. Studer, *Nano Lett.* **2001**, *1*, 281–286.